NEW AND IMPROVED CALIBRATION POINTS - THE LUNAR CRATERING CHRONOLOGY IN THE ERA OF CHANG'E, LRO, AND SELENE.

C. H. van der Bogert[1], W. Iqbal[1], H. Hiesinger[1], Y. Qian[2,3], J. W. Head[3], M. S. Robinson[4], B. L. Jolliff[5], L. Xiao[2,6], and P. Mahanti[4]; [1]Institut für Planetologie, Westfälische Wilhelms-Universität, Wilhelm-Klemm-Str. 10, 48149 Münster, Germany (vanderbogert@uni-muenster.de); [2]China University of Geosciences, Wuhan, China; [3]Brown University, Providence, Rhode Island, USA; [4]Arizona State University, Tempe, AZ 85287, USA; [5]Washington University in St. Louis, St. Louis, Missouri, USA; [6]Chinese Academy of Sciences, Hefei, China.

Introduction: The lunar cratering chronology is a tool for determining absolute model ages (AMAs) for unsampled geological units across the Moon via crater size-frequency distribution (CSFD) measurements [e.g., 1-8], and it can be modified to use on other planetary bodies [e.g. 3,4,9,10]. A chronology function (CF) is fit to a dataset portraying (1) the radio-isotopic or exposure dates for lunar samples of known provenance, and (2) the cumulative number of craters ≥ a reference diameter, typically 1 km, for the unit interpreted to represent the sample (Fig. 1). These $N(1)$ values that feed into the historical calibration were produced with Apollo and Lunar Orbiter data, and the dates for the samples were determined using older instrumental techniques. Thus, with technical advancements in instrumentation and the operation of recent lunar missions, it has been possible to begin updating each calibration point [e.g., 11-13.].

In recent years, efforts have been made to identify locations on the Moon where samples could be collected that fill the gaps in the existing calibration dataset. Suggestions have included the South Pole-Aitken basin, the young P60 basalt south of
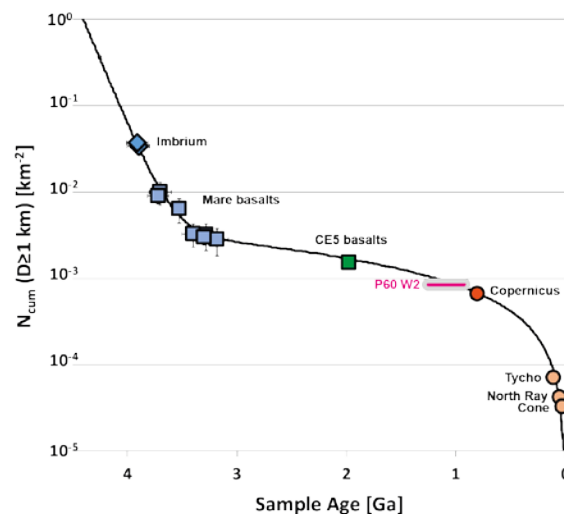

Figure 1. *The lunar cratering chronology curve (black) of Neukum (1983)[2], which is fit to radio-isotopic and exposure ages of Apollo and Luna samples and N(1) values determined for the sample units. Points with no apparent error bars have errors smaller than the size of the marker.*

Aristarchus, and the slightly older Em4/P58 basalt east of Mons Rümker [e.g., 14-18]. Thus, it was to great fanfare that the Chang'e-5 (CE5) mission was able to return samples of mare basalts from Em4/P58 at the end of 2020. The determination of radio-isotopic dates for these samples [19,20] allows the addition of a new calibration point to the lunar cratering chronology, and provides a test of the goodness of fit of the chronology function.

Here, we use our well established techniques for validating and improving chronology calibration points to review, update, and augment work done at the CE5 landing site for determining the $N(1)$ reference value. Specifically, we reexamined the count area of [21] and updated it. Then we used Lunar Reconnaissance Orbiter (LRO) Narrow Angle Camera (NAC) images to make additional CSFD measurements.

Data and Methods: For the CSFD measurements at larger crater diameters, we and Qian et al. (2021) [21] used the SELENE Terrain Camera (TC) morning mosaic (4096 pixels/degree or ~7.8 m/pixel) with an incidence angle of ~74 degrees (Haruyama et al., 2008). Here, we reviewed the crater measurements by Qian et al. (2021b) from their Area 5 (black polygon, Fig. 2), and then we adjusted the count area to exclude a wrinkle ridge along the western edge and removed more areas with secondary craters (white dashed polygon, Fig. 2). Next, we used LRO NAC mosaics to define and measure a CSFD for smaller diameter crater bins (red polygon, Fig. 2). All data were fit in cumulative form with pseudolog binning using the PF of Neukum (1983) to be consistent with historical calibration points [2,3]. We are in the process of updating each calibration point, so that the $N(1)$ values are all calculated the same way and thus build an internally consistent updated dataset.

Context and Results: Qian et al. (2021a) [21] made detailed CSFD measurements on five potential reference areas around the landing region; CE5 landed in Area 5, for which Qian et al. (2021a) [21] had determined an $N(1)$ value of 1.27 ± 0.141 x 10^{-3} km^{-2}. Our updated fits to this dataset give a somewhat higher $N(1)$ of 1.52 ± 0.078 x 10^{-3} km^{-2}, and our revised area gives a slightly higher $N(1)$ of 1.60 ± 0.081 x 10^{-3} km^{-2}. The inclusion of a wider range of crater diameters in the fit process led to the first increase. The exclusion of

the wrinkle ridge and secondary crater fields from the reference area in the next step likely causes the next increase. The exclusion of secondary crater fields, both the craters and the areas they overprint, improves the results. When we plot these $N(1)$ values against the average of the radio-isotopic dates determined for the CE5 basalt fragments [19,20], the tentative new calibration point plots just below, but within error of, the Neukum (1983) [2] chronology function (Fig. 1, green square).

When the calibration point for Copernicus crater is updated with values validated and refined by [13], the error on this point can be significantly reduced (Fig.1). Thus, when compared with the CE5 basalt, the two ages can be statistically distinguished.

Discussion: Different $N(1)$ values have been determined for the CE5 landing site and region which span a range of 1.02-1.789 (see, e.g., summary in Qiao et al., 2021 [22]). The wide spread in values can be primarily tied back to the fact that different areas of the Em4/P58 unit were selected. Qian et al. (2021b) [23] showed using a gridded count area approach, that the AMAs across the region are variable. The $N(1)$ values that we determined for the CE5 site lie in the middle of the range, and are consistent with or very similar to other work done in this particular area. For example, Morota et al. (2010) [24] also determined an $N(1)$ of 1.60×10^{-3} km^{-2}.

Implications: Our results show that the tentative new calibration point plots slightly lower than the Neukum (1983) CF. Thus, the AMAs fit with this CF slightly underestimate the radio-isotopic ages of the mare basalt at this location. On the other hand, the refined Copernicus crater point [13] is well represented by the CF, pointing to a good fit of this part of the CF to the Copernican-aged calibration points. In our ongoing work, we are validating and updating additional reference points.

References: [1] Hartmann et al. (1981) BVTP 1049-1128; [2] Neukum (1983) Habil. Thesis; [3] Neukum and Ivanov (1994) in Hazards Due to Comets and Asteroids, 359-416; [4] Neukum et al. (2001) Space Sci Rev 96, 55-86; [5] Stöffler and Ryder (2001); [6] Stöffler et al. (2006) Rev Min Geochem 60, 519-596; [7] Le Feuvre and Wieczorek (2011) ; [8] Robbins, 2014; [9] Hartmann and Neukum (2001) Space Sci Rev 96, 165-194; [10] Hiesinger et al. (2016) Science 353, 6303; [11] Hiesinger et al. (2012) JGR 117, 2011JE003935; [12] Iqbal et al. (2019) Icarus 333, 528-547; [13] Iqbal et al. (2020) Icarus 352, 113991; [14] Jolliff et al. (2012) LEAG, 3047; [15] Eldridge et al. (2010) LPSC 41, 1486; [16] Draper et al. (2021) PSJ 2, 79; [17] Anderson et al. (2015) Issues in Crater Studies, 9058; [18] Qian et al. (2018) JGR 123, 2018JE005595; [19] Che et al. (2021) Science 374, 887-890; [20] Li Q. et al., (2021) Nat Sci Rev, nwab188; [21] Qian et al., (2021) EPSL 561, 116855 ; [22] Qiao et al., (2021) GRL 48, e2021GL095132 ; [23] Qian et al. (2021) EPSL 555, 116702 ; [24] Morota et al. (2011) EPSL 302, 255-266.
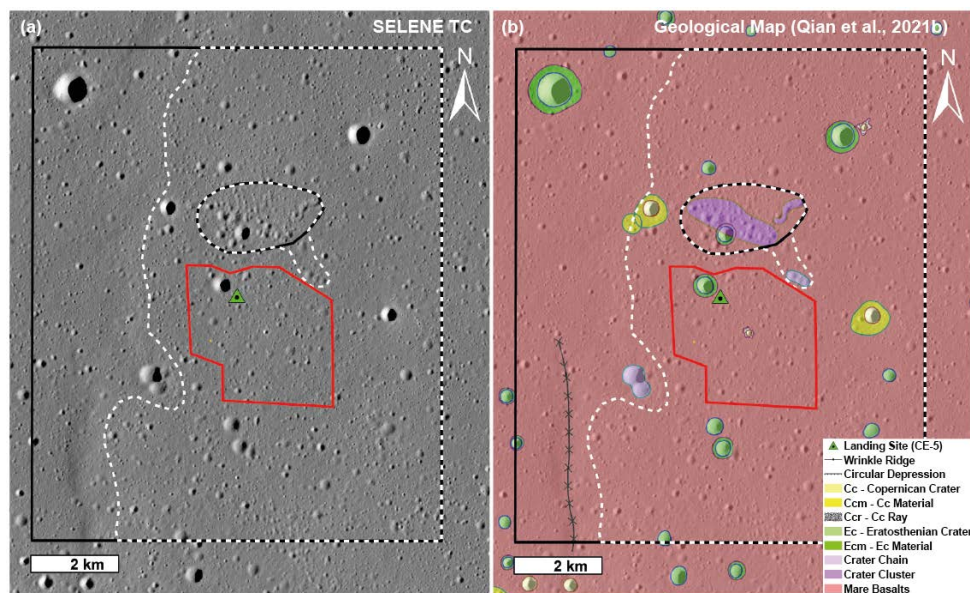

Figure 2. The region surrounding the Chang'e-5 landing site (green triangle) as shown in (a) SELENE TC data and (b) the geological map of Qian et al. (2021a) [21]. Also shown are count Area 5 of Qian et al. (2021a) [21] (black), our modified Area 5 (white dashed), and our LROC NAC count area (red).